

## Navier-Stokes numerical example

### Problem formulation

Navier-Stokes problem:

$$\left\{ \begin{array}{ll} -\nu \nabla^2 \mathbf{v} + (\mathbf{v} \cdot \nabla) \mathbf{v} + \nabla p = \mathbf{b} & \text{in } \Omega \\ \nabla \cdot \mathbf{v} = 0 & \text{in } \Omega \\ \mathbf{v} = \mathbf{v}_D & \text{on } \Gamma_D \\ \mathbf{n} \cdot \boldsymbol{\sigma} = \mathbf{t} & \text{on } \Gamma_N \end{array} \right.$$

Weak form:

$$\begin{aligned} a(\mathbf{w}, \mathbf{v}) + c(\mathbf{w}, \mathbf{v}, \mathbf{v}) + b(\mathbf{w}, p) &= (\mathbf{w}, \mathbf{b}) + (\mathbf{w}, \mathbf{t})_{\Gamma_N} \quad \forall \mathbf{w} \in \mathcal{V} \\ b(\mathbf{v}, q) &= 0 \quad \forall q \in \mathcal{Q} \end{aligned}$$

$$a(\mathbf{w}, \mathbf{v}) = \nu (\nabla \mathbf{w}, \nabla \mathbf{v})$$

$$b(\mathbf{v}, q) = -(q, \nabla \cdot \mathbf{v})$$

$$c(\mathbf{w}, \mathbf{v}, \mathbf{v}) = (\mathbf{w}, (\mathbf{v} \cdot \nabla) \mathbf{v}) = \int_{\Omega} \mathbf{w} \cdot (\mathbf{v} \cdot \nabla) \mathbf{v} \, d\Omega$$

Galerkin discretization:

$$\begin{pmatrix} \mathbf{K} + \mathbf{C}(\mathbf{v}) & \mathbf{G} \\ \mathbf{G}^T & \mathbf{0} \end{pmatrix} \begin{pmatrix} \mathbf{u} \\ \mathbf{p} \end{pmatrix} = \begin{pmatrix} \mathbf{f} \\ \mathbf{h} \end{pmatrix}$$

### Discretization of the convective term for the Piccard's method

The following code shows the discretization for the linearized form of the convection matrix on the element level.

```
function [C] = ConvectionMatrix(X,T,referenceElement , velo)
...
    v_igaus = N_ig*u_e;
    Ce = Ce + Ngp'*(v_igaus(1)*Nx+v_igaus(2)*Ny)*dvolu;
...
end
```

## Discretization of the Newton-Raphson scheme

The following code shows the discretization for the linearized form of the convection matrix on the element level.

```
function [C1,C2] = ConvectionMatrix(X,T,referenceElement ,velo)
...
    v_igaus = N_ig*u_e;
    Ce1 = Ce1 + Ngp'*(v_igaus(1)*Nx+v_igaus(2)*Ny)*dvolu;
    Ce2 = Ce2 + Ngp'*([nx ; ny]*u_e) '*Ngp*dvolu;
...
```

The following code shows the implementation of the Newton-Raphson algorithm in the file `mainNavierStokes.m`:

```
...
    [C1,C2] = ConvectionMatrixNR(X,T,referenceElement ,velo);
    Cred1 = C1(dofUnk ,dofUnk);
    Cred2 = C2(dofUnk ,dofUnk);

    A = [Kred + Cred1   Gred';
         Gred   zeros(nunkP)];

    Atot = A;
    btot = [fred - (C1(dofUnk ,dofDir))*valDir; zeros(nunkP,1)];

    J = [Kred + Cred1 + Cred2   Gred';
         Gred   zeros(nunkP)];

    F = Atot*sol0 - btot;

    % Computation of velocity and pressure increment

    solInc =-J\F;

    % Update the solution
    veloInc = zeros(ndofV,1);
    veloInc(dofUnk) = solInc(1:nunkV);
    presInc = solInc(nunkV+1:end);
    velo = velo + reshape(veloInc,2,[],)';
    pres = pres + presInc;
...
```

## Results and convergence study

To compare the Piccard's method with the Newton-Raphson scheme the cavity flow problem was computed with quadrilateral elements (Q2Q1). Figure 1 and Figure 2 show that in both cases the solution is stable. As expected, it is hard to see any differences with respect to the accuracy of the results. A distinctive property of the two methods becomes only visible when looking at the convergence plots in Figure 3 where the residual  $F$  is plotted against the number of iterations. For the Piccard's scheme a linear relation between the error estimate and the number of iteration can be observed. The Newton-Raphson method on the other hand shows a quadratic behaviour.

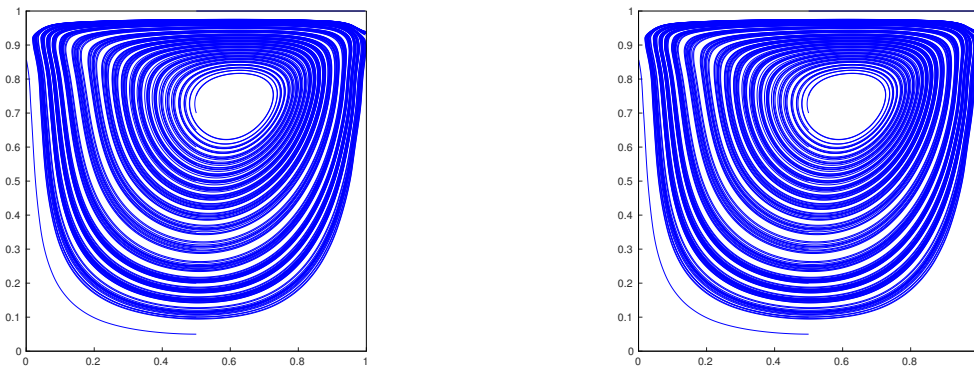


Figure 1: Streamlines for the Q2Q1 element obtained with Piccard's (left) and Newton-Raphson (right) scheme

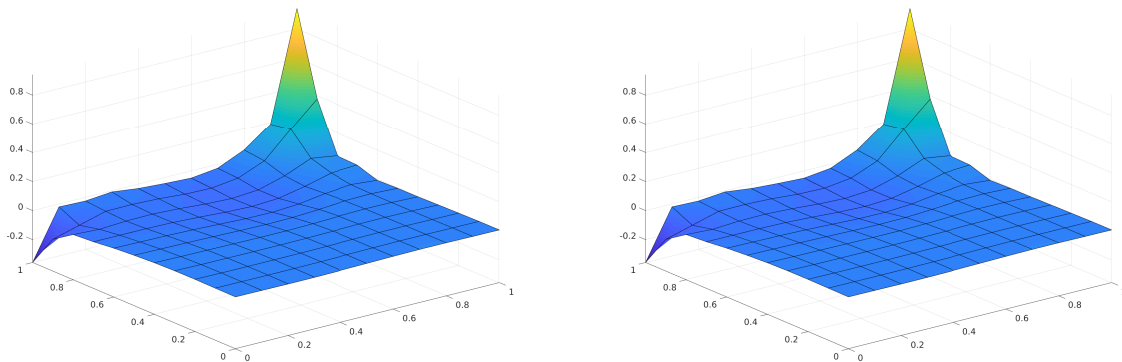


Figure 2: Streamlines for the Q2Q1 element obtained with Piccard's (left) and Newton-Raphson (right) scheme

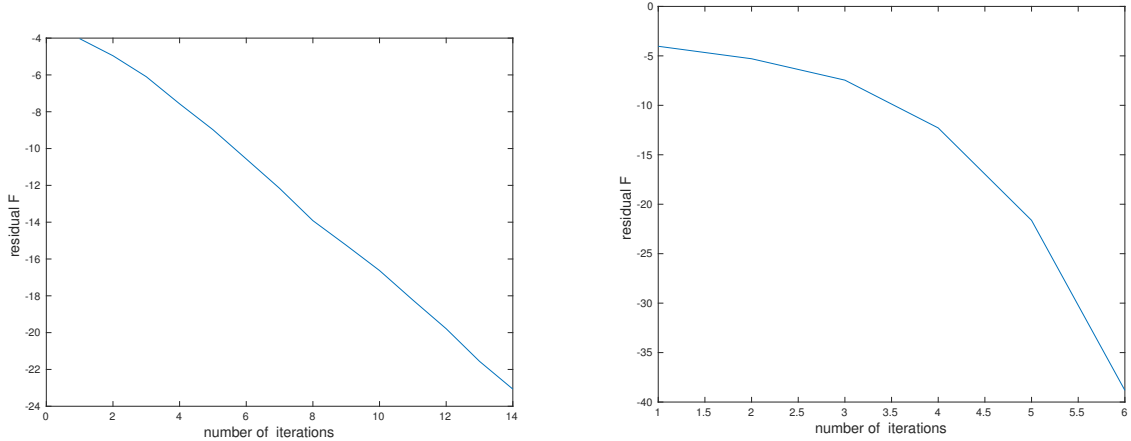


Figure 3: Convergence plots for the Piccard's scheme (left) and the Newton-Raphson scheme (right)